Advances in Nano Research, *Vol. 9, No. 1 (2020) 47-58*
DOI: https://doi.org/10.12989/anr.2020.9.1.047

Analyzing exact nonlinear forced vibrations of two-phase magneto-electro-elastic nanobeams under an elliptic-type force

Seyed Sajad Mirjavadi [1], Mohammad Nikookar [2], Saeed Mollaee [3],
Masoud Forsat*[1], Mohammad Reza Barati [4] and A.M.S. Hamouda [1]

[1] *Department of Mechanical and Industrial Engineering, Qatar University, P.O. Box 2713, Doha, Qatar*
[2] *Department of Civil Engineering, Faculty of Engineering, University of Guilan, Rasht, Iran*
[3] *Auckland Bioengineering Institute, University of Auckland, Auckland, New Zealand*
[4] *Fidar project Qaem Company, Darvazeh Dolat, Tehran, Iran*

(*Received January 31, 2020, Revised April 19, 2020, Accepted May 20, 2020*)

Abstract. The present paper deals with analyzing nonlinear forced vibrational behaviors of nonlocal multi-phase piezo-magnetic beam rested on elastic substrate and subjected to an excitation of elliptic type. The applied elliptic force may be presented as a Fourier series expansion of Jacobi elliptic functions. The considered multi-phase smart material is based on a composition of piezoelectric and magnetic constituents with desirable percentages. Additionally, the equilibrium equations of nanobeam with piezo-magnetic properties are derived utilizing Hamilton's principle and von-Kármán geometric nonlinearity. Then, an exact solution based on Jacobi elliptic functions has been provided to obtain nonlinear vibrational frequencies. It is found that nonlinear vibrational behaviors of the nanobeam are dependent on the magnitudes of induced electrical voltages, magnetic field intensity, elliptic modulus, force magnitude and elastic substrate parameters.

Keywords: forced vibration; piezo-magnetic material; nonlinear vibrations; piezoelectric reinforcement; nonlocal elasticity

1. Introduction

Recently, the development in the field of engineering materials has disclosed the advantages associated with the smart/intelligent materials. Incorporation of these smart materials in various multifunctional structures has paved way for tremendous changes in different engineering fields (Mahesh *et al*. 2018, 2019, Mirjavadi *et al*. 2017, 2018a, b, 2019a, b, c, Azimi *et al*. 2017, 2018). Among them, magneto-electro-elastic (MEE) materials are unique as a matter of fact that it exhibits triple energy conversion between elastic, electrical and magnetic fields (Pan and Han 2005, Mahesh and Kattimani 2019). Therefore, it has become a potential candidate for sophisticated applications such as vibration control (Li and Shi 2009, Guo *et al*. 2016), energy harvesting, sensors and actuators etc (Vinyas and Kattimani 2017a, b, c, d, 2018, Vinyas *et al*. 2019, 2020, Vinyas 2020a, b, c). More recently, attempts were made to synthesize MEE structures through composite materials and improvise the structural functionalities. For example, the mechanical characteristics of multi-phase MEE materials may be controlled via the variation of material composition and portion of each phase (Nan 1994). Having realized that the smart structures made of magneto-electro-elastic materials with different material composition play a significant role in industrial fields many pioneers have devoted their research to access the mechanical response in various working environments (Kumaravel *et al*. 2007, Annigeri *et al*. 2007, Chaudhary *et al*. 2017, Semmah *et al*. 2019).

At nano range, significant influence of size effects is noticed on both physical as well as the mechanical properties. This phenomenon has motivated few researchers to divert their focus towards assessing the mechanical response of the nanostructures. The major limitation of the classical continuum mechanics is its inefficiency to model small size structures which paved way for the establishment of higher order continuum theories which incorporates the size dependency of structure with ease (Barati 2017, Aydogdu *et al*. 2018, Benmansour *et al*. 2019, Yazid *et al*. 2018, Mokhtar *et al*. 2018, Ahmed *et al*. 2019, Al-Maliki *et al*. 2019, Fenjan *et al*. 2019). The Eringen's nonlocal elasticity theory (Eringen 1972) proved to be handy in employing the size-effects. Due to the reason that performing experiment on a nano-size structure is still hard, many articles have been published to make the best utilization of this theory in evaluating the size-dependent structural response (Thai and Vo 2012, Eltaher *et al*. 2012, Zemri *et al*. 2015, Bounouara *et al*. 2016, Akbas 2016, Besseghier *et al*. 2015, Mouffoki *et al*. 2017, Berghouti *et al*. 2019). The major outcome these researches indicate that with the higher value of nonlocal parameter, that nonlocal elastic models are efficient enough only to yield stiffness-softening effect. Incorporating the Eringen's nonlocal elasticity theory few researchers attempted to analyze the MEE or piezo-magnetic nanostructures. Ke *et al*. (2014) examined linear free vibrations of MEE cylindrical

*Corresponding author, Ph.D., Professor,
E-mail: masoudforsatlar@gmail.com

http://www.techno-press.org/?journal=journal=anr&subpage=5
ISSN: 2287-237X (Print), 2287-2388 (Online)

nanoshells via a numerical approach. Ebrahimi and Barati (2016) explored nonlocal small-amplitude vibrations of MEE nanobeams having viscoelastic properties. Farajpour *et al*. (2016) studied nonlinear vibrational behavior of a MEE nano-dimension plate via an analytical solution. Liu *et al*. (2018) researched vibration behavior of MEE nanobeams with functionally graded properties resting on visco-elastic foundation. Dehghan and Ebrahimi (2018) studied wave propagation in nanoshells taking into account nonlocal effects. In above works on MEE nanostructures, the authors did not consider the effect of different piezoelectric phase percentages (material composition).

Up to now, many solution methods are introduced in the literature in order to solve nonlinear vibration problem of structures, especially nano-dimension structures. Most of these methods provide an approximate solution for the problem leading to a closed-form of vibration frequency (She *et al*. 2018, Alasadi *et al*. 2019). Most of these methods consider only the first harmonic in the solution procedure and this means that the solution is not exact. For improving the accuracy of solution, higher order harmonics must be added which makes the solution procedure difficult. Exact solution of the nonlinear equations of a vibrating structure can be found based on Jacobi elliptic functions (Liu *et al*. 2001). Such functions represent a more general class of periodic functions, which include trigonometric functions as a specific case. Further discussions on these functions are available in following sections.

In view of the above, the aim of the present article is to develop a multi-phase MEE nanobeam resting on nonlinear elastic substrate under an excitation of elliptic type for forced vibration analysis within the framework of nonlocal elasticity theory. It is supposed that the MEE composite has two phases with piezoelectric and magnetic constituents. Eringen's elasticity theory is served to study the nano-scale effect. Additionally, the equilibrium equations of nanobeam with MEE properties are derived utilizing Hamilton's principle and von-Kármán geometric nonlinearity. Then, an exact solution based on Jacobi elliptic functions has been provided with high accuracy. A parametrical study is carried out to examine the influence of nonlocality, various piezoelectric volume, electro-magnetic field, elastic substrate coefficients, elliptic modulus and force magnitude on the structural performance of such nano-scale systems. The results of this paper can be a good reference for designing and optimizing the smart structures under dynamic loads.

2. Two-phase composite of magneto-electro-elastic type

Fig. 1 indicates a nano-scale beam made of magneto-electro-elastic composite with two phases. Material properties of multi-phase MEE composite rely on the percentage and volume of piezoelectric phase (V_f). This article studies a nanobeam constructed by a composite of $BaTiO_3$-$CoFe_2O_4$ for which Table 1 is devoted to represent the material properties. For such materials, $BaTiO_3$ denotes the piezo-electrical ingredient and also $CoFe_2O_4$ denotes the piezo-magnetic ingredient. Based on Table 1, elastic (C_{ij}), piezo-electrical (e_{ij}) and magneto-electric (q_{ij}) parameters have been presented. Furthermore, k_{ij}, d_{ij} and x_{ij} indicate the dielectric, magneto-electrical and magnetic permeability coefficients, respectively.

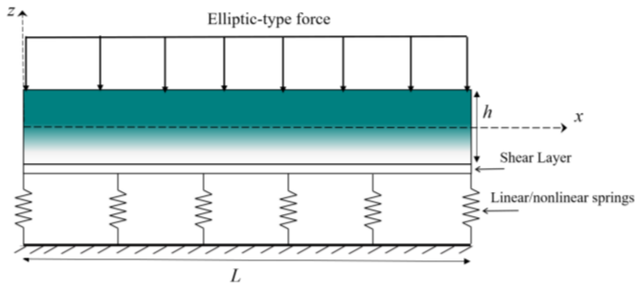

Fig. 1 A piezo-magnetic composite nanobeam rested on elastic substrate

Table 1 Material constants for $BaTiO_3$-$CoFe_2O_4$ composite

Property	$V_f = 0$	$V_f = 0.2$	$V_f = 0.4$	$V_f = 0.6$	$V_f = 0.8$
C_{11} (GPa)	286	250	225	200	175
C_{13}	170	145	125	110	100
C_{33}	269.5	240	220	190	170
e_{31} (C/m^2)	0	-2	-3	-3.5	-4
e_{33}	0	4	7	11	14
q_{31} (N/Am)	580	410	300	200	100
q_{33}	700	550	380	260	120
k_{11} (10^{-9} Vm)	0.08	0.33	0.8	0.9	1
k_{33}	0.093	2.5	5	7.5	10
d_{11} (10^{-12} Ns/VC)	0	2.8	4.8	6	6.8
d_{33}	0	2000	2750	2500	1500
x_{11} (10^{-4} Ns^2/C^2)	-5.9	-3.9	-2.5	-1.5	-0.8
x_{33}	1.57	1.33	1	0.75	0.5
ρ (kg/m^3)	5300	5400	5500	5600	5700

3. Mathematical formulation

So far, different beam and plate theories are available in the literature (Abualnour *et al*. 2019, Bedia *et al*. 2019, Addou *et al*. 2019, Alimirzaei *et al*. 2019, Balubaid *et al*. 2019, Batou *et al*. 2019, Belbachir *et al*. 2019, Chaabane *et al*. 2019, Draiche *et al*. 2019, Draoui *et al*. 2019, Hussain *et al*. 2019, Hellal *et al*. 2019, Boutaleb *et al*. 2019, Bourada *et al*. 2019, Boulefrakh *et al*. 2019, Mahmoudi *et al*. 2019, Meksi *et al*. 2019, Medani *et al*. 2019, Tlidji *et al*. 2019, Zarga *et al*. 2019, Zaoui *et al*. 2019, Sahla *et al*. 2019, Boukhlif *et al*. 2019, Kaddari *et al*. 2020). In this section, the procedure of obtaining governing equations for a piezo-magnetic nanobeam will be presented in the context of nonlocal and classic beam theories. For achieving this goal, the displacement field of nano-scale beam based on axial (u) and transverse (w) displacements at the mid-axis may be written as

$$u_1(x,y,z,t) = u(x,y,t) - z\frac{\partial w}{\partial x} \tag{1}$$

$$u_3(x,y,z,t) = w(x,y,t) \tag{2}$$

For considering geometric nonlinearity, the axial strain of the beam should be written as (Alasadi *et al*. 2019).

$$\varepsilon_{xx} = \frac{\partial u_1}{\partial x} = \frac{\partial u}{\partial x} - z\frac{\partial^2 w}{\partial x^2} + \frac{1}{2}(\frac{\partial w}{\partial x})^2 \tag{3}$$

In this research, it is supposed that electric voltage (V_E) and magnetic field intensity (Ω) due to magnetic $\Upsilon(x,z,t)$ and electrical $\Phi(x,z,t)$ field potentials are applied to the nano-size beam. The potentials can be expressed in the form (Ebrahimi and Barati 2016)

$$\Phi(x,y,z,t) = -\cos(\beta z)\phi(x,y,t) + \frac{2z}{h}V_E \tag{4}$$

$$\Upsilon(x,y,z,t) = -\cos(\beta z)\gamma(x,y,t) + \frac{2z}{h}\Omega \tag{5}$$

where $\beta = \pi/h$. Above potentials lead to induction of electrical field (E_x, E_z) and magnetic field (H_x, H_z) in x and z directions which can be derived via Eqs. (4) and (5) as

$$\begin{aligned} E_x &= -\Phi_{,x} = \cos(\beta z)\frac{\partial \phi}{\partial x} \\ E_z &= -\Phi_{,z} = -\beta \sin(\beta z)\,\phi - \frac{2V_E}{h} \end{aligned} \tag{6}$$

$$\begin{aligned} H_x &= -\Upsilon_{,x} = \cos(\beta z)\frac{\partial \gamma}{\partial x} \\ H_z &= -\Upsilon_{,z} = -\beta \sin(\beta z)\,\gamma - \frac{2\Omega}{h} \end{aligned} \tag{7}$$

There are four coupled governing equations for a multi-phase piezo-magnetic nano-size beam embedded on elastic substrate which can be derived via Hamilton's principle as (Fenjan *et al*. 2019).

$$\frac{\partial N_x}{\partial x} = I_0\frac{\partial^2 u}{\partial t^2} - I_1\frac{\partial^3 w}{\partial x \partial t^2} \tag{8}$$

$$\begin{aligned} &\frac{\partial^2 M_x}{\partial x^2} + \frac{\partial}{\partial x}N_x\left(\frac{\partial w}{\partial x}\right) - k_L w + k_P\frac{\partial^2 w}{\partial x^2} - k_{NL}w^3 \\ &= I_0\frac{\partial^2 w}{\partial t^2} + I_1(\frac{\partial^3 u}{\partial x \partial t^2}) - I_2\nabla^2(\frac{\partial^2 w}{\partial t^2}) + q_{elliptic} \end{aligned} \tag{9}$$

$$\int_{-h/2}^{h/2}\left(\cos(\beta z)\frac{\partial D_x}{\partial x} + \beta \sin(\beta z)\,D_z\right)dz = 0 \tag{10}$$

$$\int_{-h/2}^{h/2}\left(\cos(\beta z)\frac{\partial B_x}{\partial x} + \beta \sin(\beta z)\,B_z\right)dz = 0 \tag{11}$$

The elliptic force can be defined in the form $q_{elliptic} = Fcn(\psi t, k_f^2)$ which has the magnitude of F, excitation frequency ψ and the modulus of elliptic function k_f.

Also, D_i and B_i display the displacement components of electrical and magnetic fields; k_L, k_P, k_{NL} display linear, shear and non-linear coefficients of elastic layer.

Furthermore, N_x and M_x are corresponding to in-plane forces and bending moments which can be defined by

$$(N_x, M_x) = \int_A (1,z)\sigma_x\, dA \tag{12}$$

$$(I_0, I_1, I_2) = \int_{-h/2}^{h/2}(1,z,z^2)\rho\, dz \tag{13}$$

Knowing the fact that considered material is isotropic, one can reach to $I_1 = 0$. Next, derived boundary conditions may be denoted by

$$N_x = 0 \quad or \quad u = 0 \tag{14}$$

$$\frac{\partial M_x}{\partial x} + N_x\left[\frac{\partial w}{\partial x}\right] = 0 \quad or \quad w = 0 \tag{15}$$

$$\int_{-h/2}^{h/2}\cos(\beta z)\,D_x dz = 0 \quad or \quad \phi = 0 \tag{16}$$

$$\int_{-h/2}^{h/2}\cos(\beta z)\,B_x dz = 0 \quad or \quad \gamma = 0 \tag{17}$$

Introducing nonlocal parameter ea^2, the constitutive relations for a nano-size piezo-magnetic beam should be written in the following forms.

$$(1-(ea)^2\nabla^2)\sigma_{xx} = \tilde{c}_{11}\varepsilon_{xx} - \tilde{e}_{31}E_z - \tilde{q}_{31}H_z \tag{18}$$

$$(1-(ea)^2\nabla^2)D_x = \tilde{e}_{15}\gamma_{xz} + \tilde{k}_{11}E_x + \tilde{d}_{11}H_x \tag{19}$$

$$(1-(ea)^2\nabla^2)D_z = \tilde{e}_{31}\varepsilon_{xx} + \tilde{k}_{33}E_z + \tilde{d}_{33}H_z \tag{20}$$

$$(1-(ea)^2\nabla^2)B_x = \tilde{q}_{15}\gamma_{xz} + \tilde{d}_{11}E_x + \tilde{\chi}_{11}H_x \tag{21}$$

$$(1-(ea)^2\nabla^2)B_z = \tilde{q}_{31}\varepsilon_{xx} + \tilde{d}_{33}E_z + \tilde{\chi}_{33}H_z \tag{22}$$

where $\tilde{c}_{ij}$, $\tilde{e}_{ij}$, $\tilde{q}_{ij}$, $\tilde{d}_{ij}$, $\tilde{k}_{ij}$ and $\tilde{\chi}_{ij}$ illustrate modified properties for plane stress state

$$\begin{aligned} &\tilde{c}_{11} = c_{11} - \frac{c_{13}^2}{c_{33}}, \quad \tilde{c}_{12} = c_{12} - \frac{c_{13}^2}{c_{33}}, \quad \tilde{c}_{66} = c_{66}, \\ &\tilde{e}_{15} = e_{15}, \quad \tilde{e}_{31} = e_{31} - \frac{c_{13}e_{33}}{c_{33}}, \\ &\tilde{q}_{15} = q_{15}, \quad \tilde{q}_{31} = q_{31} - \frac{c_{13}q_{33}}{c_{33}}, \\ &\tilde{d}_{11} = \tilde{d}_{11}, \quad \tilde{d}_{33} = \tilde{d}_{33} + \frac{q_{33}e_{33}}{c_{33}}, \\ &\tilde{k}_{11} = k_{11}, \quad \tilde{k}_{33} = k_{33} + \frac{e_{33}^2}{c_{33}}, \\ &\tilde{\chi}_{11} = \chi_{11}, \quad \tilde{\chi}_{33} = \chi_{33} + \frac{q_{33}^2}{c_{33}} \end{aligned} \tag{23}$$

Integrating the constitutive equations represented in Eqs. (18)-(22) according to the thickness, the below expressions can be derived for a nano-size piezo-magnetic beam.

$$(1-(ea)^2\nabla^2)N_x = A_{11}\left(\frac{\partial u}{\partial x}+\frac{1}{2}\left(\frac{\partial w}{\partial x}\right)^2\right) \\ -B_{11}\frac{\partial^2 w}{\partial x^2}+A_{31}^e\phi+A_{31}^m\gamma-N_x^E-N_x^H \tag{24}$$

$$(1-(ea)^2\nabla^2)M_x = B_{11}\left(\frac{\partial u}{\partial x}+\frac{1}{2}\left(\frac{\partial w}{\partial x}\right)^2\right) \\ -D_{11}\frac{\partial^2 w}{\partial x^2}+E_{31}^e\phi+E_{31}^m\gamma-M_x^E-M_x^H \tag{25}$$

$$\int_{-\frac{h}{2}}^{\frac{h}{2}}(1-(ea)^2\nabla^2)D_x\cos(\beta z)\,dz \\ = F_{11}^e\frac{\partial\phi}{\partial x}+F_{11}^m\frac{\partial\gamma}{\partial x} \tag{26}$$

$$(1-(ea)^2\nabla^2)\int_{-\frac{h}{2}}^{\frac{h}{2}}D_z\beta\sin(\beta z)\,dz \\ = A_{31}^e\left(\frac{\partial u}{\partial x}+\frac{1}{2}\left(\frac{\partial w}{\partial x}\right)^2\right)-E_{31}^e\frac{\partial^2 w}{\partial x^2}-F_{33}^e\phi-F_{33}^m\gamma \tag{27}$$

$$\int_{-\frac{h}{2}}^{\frac{h}{2}}(1-(ea)^2\nabla^2)B_x\cos(\beta z))dz \\ = +F_{11}^m\frac{\partial\phi}{\partial x}+X_{11}^m\frac{\partial\gamma}{\partial x} \tag{28}$$

$$\int_{-\frac{h}{2}}^{\frac{h}{2}}(1-(ea)^2\nabla^2)B_z\beta\sin(\beta z))dz \\ = A_{31}^m\left(\frac{\partial u}{\partial x}+\frac{1}{2}\left(\frac{\partial w}{\partial x}\right)^2\right)-E_{31}^m\nabla^2 w-F_{33}^m\phi\;-X_{33}^m\gamma \tag{29}$$

so that

$$\{A_{11},B_{11},D_{11}\}=\int_{-h/2}^{h/2}\tilde{c}_{11}(1,z,z^2)\,dz \tag{30}$$

$$\{A_{31}^e,E_{31}^e\}=\int_{-h/2}^{h/2}\tilde{e}_{31}\beta\sin(\beta z)\{1,z\}\,dz \tag{31}$$

$$\{A_{31}^m,E_{31}^m\}=\int_{-h/2}^{h/2}\tilde{q}_{31}\beta\sin(\beta z)\{1,z\}\,dz \tag{32}$$

$$\{F_{11}^e,F_{33}^e\}=\int_{-h/2}^{h/2}\{\tilde{k}_{11}\cos^2(\beta z),\tilde{k}_{33}\beta^2\sin^2(\beta z)\}\,dz \tag{33}$$

$$\{F_{11}^m,F_{33}^m\}=\int_{-h/2}^{h/2}\{\tilde{d}_{11}\cos^2(\beta z),\tilde{d}_{33}\beta^2\sin^2(\beta z)\}\,dz \tag{34}$$

$$\{X_{11}^m,X_{33}^m\}=\int_{-h/2}^{h/2}\{\tilde{\chi}_{11}\cos^2(\beta z),\tilde{\chi}_{33}\beta^2\sin^2(\beta z)\}\,dz \tag{35}$$

Applied electro-magnetic force and moments provided in Eqs. (24)-(25) can be defined as follows.

$$N_x^E=-\int_{-\frac{h}{2}}^{\frac{h}{2}}\tilde{e}_{31}\frac{2V}{h}dz\,, \\ N_x^H=-\int_{-h/2}^{h/2}\tilde{q}_{31}\frac{2\Omega}{h}dz \tag{36}$$

$$M_x^E=-\int_{-\frac{h}{2}}^{\frac{h}{2}}\tilde{e}_{31}\frac{2V}{h}zdz\,, \\ M_x^H=-\int_{-h/2}^{h/2}\tilde{q}_{31}\frac{2\Omega}{h}zdz \tag{37}$$

Four governing equations presented as Eqs. (8)-(11) can be represented in terms of displacements by placing Eqs. (24)-(29) in them as

$$A_{11}\left(\frac{\partial^2 u}{\partial x^2}+\frac{\partial w}{\partial x}\frac{\partial^2 w}{\partial x^2}\right) \\ -B_{11}\frac{\partial^3 w}{\partial x^3}+A_{31}^e\frac{\partial\phi}{\partial x}+A_{31}^m\frac{\partial\gamma}{\partial x}=0 \tag{38}$$

$$-D_{11}\frac{\partial^4 w}{\partial x^4}+E_{31}^e\left(\frac{\partial^2\phi}{\partial x^2}\right)+E_{31}^m\left(\frac{\partial^2\gamma}{\partial x^2}\right)(1-(ea)^2\nabla^2) \\ \left(-I_0\frac{\partial^2 w}{\partial t^2}-I_1\left(\frac{\partial^3 u}{\partial x\partial t^2}\right)+I_2\left(\frac{\partial^4 w}{\partial x^2\partial t^2}\right)\right. \\ +\left(A_{11}\left(\frac{\partial u}{\partial x}+\frac{1}{2}\left(\frac{\partial w}{\partial x}\right)^2\right)B_{11}\frac{\partial^2 w}{\partial x^2}+A_{31}^e\phi+A_{31}^m\gamma\right. \\ \left.-N_x^E-N_x^H\right)\left[\frac{\partial^2 w}{\partial x^2}\right]+(1-(ea)^2\nabla^2) \\ \left(-k_L w+k_P\frac{\partial^2 w}{\partial x^2}-k_{NL}w^3\right)=(1-(ea)^2\nabla^2)q_{elliptic} \tag{39}$$

$$A_{31}^e\left(\frac{\partial u}{\partial x}+\frac{1}{2}\left(\frac{\partial w}{\partial x}\right)^2+\frac{\partial w}{\partial x}\frac{\partial w^*}{\partial x}\right)-E_{31}^e\left(\frac{\partial^2 w}{\partial x^2}\right) \\ +F_{11}^e\left(\frac{\partial^2\phi}{\partial x^2}\right)+F_{11}^m\left(\frac{\partial^2\gamma}{\partial x^2}\right)-F_{33}^e\phi-F_{33}^m\gamma=0 \tag{40}$$

$$A_{31}^m\left(\frac{\partial u}{\partial x}+\frac{1}{2}\left(\frac{\partial w}{\partial x}\right)^2+\frac{\partial w}{\partial x}\frac{\partial w^*}{\partial x}\right)-E_{31}^m\left(\frac{\partial^2 w}{\partial x^2}\right) \\ +F_{11}^m\left(\frac{\partial^2\phi}{\partial x^2}\right)+X_{11}^m\left(\frac{\partial^2\gamma}{\partial x^2}\right)-F_{33}^m\phi-X_{33}^m\gamma=0 \tag{41}$$

It is also possible to reduce the number of above governing equations to three equation by deriving $\partial u/\partial x$ from Eq. (38) and then substituting it in Eqs. (39)-(41). Thus, knowing this fact that axial inertia has negligible impact on transversal vibrations, Eq. (38) becomes

$$A_{11}\left(\frac{\partial u}{\partial x}+\frac{1}{2}\left(\frac{\partial w}{\partial x}\right)^2\right) \\ +A_{31}^e\phi+A_{31}^m\gamma-N_x^E-N_x^H=C_1 \tag{42}$$

Then

$$\frac{\partial u}{\partial x}=-\frac{1}{2}\left(\frac{\partial w}{\partial x}\right)^2-\frac{A_{31}^e}{A_{11}}\phi-\frac{A_{31}^m}{A_{11}}\gamma+\frac{N_x^E}{A_{11}}+\frac{N_x^H}{A_{11}}+\frac{C_1}{A_{11}} \quad (43)$$

Next, integrating Eq. (43) yields

$$\begin{aligned} u=&-\frac{1}{2}\int_0^x\left(\frac{\partial w}{\partial x}\right)^2 dx-\frac{A_{31}^e}{A_{11}}\int_0^x\phi\,dx-\frac{A_{31}^m}{A_{11}}\int_0^x\gamma\,dx\\ &+\frac{N_x^E}{A_{11}}\int_0^x dx+\frac{N_x^H}{A_{11}}\int_0^x dx+\frac{C_1}{A_{11}}x+C_2 \end{aligned} \quad (44)$$

Then, by satisfying edge conditions $u(0) = 0$, $u(L) = 0$, one can derive

$$\begin{aligned} &C_2=0\\ &C_1=\frac{A_{11}}{2L}\int_0^L\left(\frac{\partial w}{\partial x}\right)^2 dx+\frac{A_{31}^e}{L}\int_0^L\phi\,dx\\ &\quad+\frac{A_{31}^m}{L}\int_0^L\gamma\,dx-(N_x^E+N_x^H) \end{aligned} \quad (45)$$

As the next step, finded constant must be situated in Eq. (44). Accordingly, the governing equations take the following forms.

$$\begin{aligned} &-D_{11}\frac{\partial^4 w}{\partial x^4}+E_{31}^e\left(\frac{\partial^2\phi}{\partial x^2}\right)+E_{31}^m\left(\frac{\partial^2\gamma}{\partial x^2}\right)\\ &+(1-(ea)^2\nabla^2)\left(-I_0\frac{\partial^2 w}{\partial t^2}-I_1\left(\frac{\partial^3 u}{\partial x\partial t^2}\right)\right.\\ &+I_2\left(\frac{\partial^4 w}{\partial x^2\partial t^2}\right)+\left(A_{11}\left(\frac{1}{2L}\int_0^L\left(\frac{\partial w}{\partial x}\right)^2 dx\right)\right.\\ &\left.\left.-B_{11}\frac{\partial^2 w}{\partial x^2}-N_x^E-N_x^H\right)\right)\left[\frac{\partial^2 w}{\partial x^2}\right]\\ &+(1-(ea)^2\nabla^2)\left(-k_L w+k_P\frac{\partial^2 w}{\partial x^2}-k_{NL}w^3\right)\\ &=(1-(ea)^2\nabla^2)q_{elliptic} \end{aligned} \quad (46)$$

$$\begin{aligned} &A_{31}^e\left(-\frac{A_{31}^e}{A_{11}}\phi-\frac{A_{31}^m}{A_{11}}\gamma+\frac{1}{2L}\int_0^L\left(\frac{\partial w}{\partial x}\right)^2 dx\right)\\ &-E_{31}^e\left(\frac{\partial^2 w}{\partial x^2}\right)+F_{11}^e\left(\frac{\partial^2\phi}{\partial x^2}\right)+F_{11}^m\left(\frac{\partial^2\gamma}{\partial x^2}\right)\\ &-F_{33}^e\phi-F_{33}^m\gamma=0 \end{aligned} \quad (47)$$

$$\begin{aligned} &A_{31}^m\left(-\frac{A_{31}^e}{A_{11}}\phi-\frac{A_{31}^m}{A_{11}}\gamma+\frac{1}{2L}\int_0^L\left(\frac{\partial w}{\partial x}\right)^2 dx\right)\\ &-E_{31}^m\left(\frac{\partial^2 w}{\partial x^2}\right)+F_{11}^m\left(\frac{\partial^2\phi}{\partial x^2}\right)+X_{11}^m\left(\frac{\partial^2\gamma}{\partial x^2}\right)\\ &-F_{33}^m\phi-X_{33}^m\gamma=0 \end{aligned} \quad (48)$$

4. Method of solution

In this part, by employing Galerkin's approach, the governing equations of motion for free vibrations of simply-supported MEE nano-size beam have been solved. The displacement functions are provided as product of non-unknown coefficients and known trigonometric functions to assure the boundary conditions at $x = 0$ and $x = L$ as (Fenjan *et al.* 2019).

$$w=\sum_{m=1}^{\infty}W_m(t)X_m(x) \quad (49)$$

$$\phi=\sum_{m=1}^{\infty}\Phi_m(t)X_m(x) \quad (50)$$

$$\gamma=\sum_{m=1}^{\infty}\Upsilon_m(t)X_m(x) \quad (51)$$

where (W_m, Φ_m, γ_m) display the field largest values and the function $X_m = sin(m\pi x/L)$ displays the shape function of simply supported beam ($w=\frac{\partial^2 w}{\partial x^2}=\gamma=\phi=0$). Applying the functions X_m to the mentioned conditions shows the reliability of the functions in satisfying boundary conditions.

Placing Eqs. (49)-(51) in Eqs. (46)-(48) yields below equations.

$$\begin{aligned} &K_1^S W_m+G_1W_m^3+Q_1W_m^2+M\ddot{W}_m\\ &\quad+K_1^E\Phi_m+K_1^H\Upsilon_m=Fcn(\psi t,k_f^2)\\ &K_2^S W_m+G_2W_m^2+K_2^E\Phi_m+K_2^H\Upsilon_m=0\\ &K_3^S W_m+G_3W_m^2+K_3^E\Phi_m+K_3^H\Upsilon_m=0 \end{aligned} \quad (52)$$

in which

$$\begin{aligned} K_1^S=&-D_{11}(\Lambda_{40})-k_w\Lambda_{00}+k_p\Lambda_{20}\\ &-(N_x^E+N_x^H)\Lambda_{20}+(ea)^2(N_x^E+N_x^H)\Lambda_{40} \end{aligned} \quad (53)$$

$$\begin{aligned} G_1=&\frac{A_{11}}{2L}\Lambda_{11}\Lambda_{20}-(ea)^2\frac{A_{11}}{2L}\Lambda_{11}\Lambda_{40}\\ &-k_{nl}(\Lambda_{0000}-(ea)^2(\Lambda_{1100}+\Lambda_{2000})) \end{aligned} \quad (54)$$

$$K_1^E=E_{31}^e\Lambda_{20} \quad (55)$$

$$K_1^H=E_{31}^m\Lambda_{20} \quad (56)$$

$$K_2^S=-E_{31}^e\Lambda_{20} \quad (57)$$

$$K_3^S=-E_{31}^m\Lambda_{20} \quad (58)$$

$$G_2=\frac{A_{31}^e}{2L}\Lambda_0\Lambda_{11} \quad (59)$$

$$G_3=\frac{A_{31}^m}{2L}\Lambda_0\Lambda_{11} \quad (60)$$

$$K_2^E=-\frac{(A_{31}^e)^2}{A_{11}}\Lambda_{00}+F_{11}^e\Lambda_{20}-F_{33}^e\Lambda_{00} \quad (61)$$

$$K_2^H=-\frac{A_{31}^eA_{31}^m}{A_{11}}\Lambda_{00}+F_{11}^m\Lambda_{20}-F_{33}^m\Lambda_{00} \quad (62)$$

$$K_3^E=-\frac{A_{31}^eA_{31}^m}{A_{11}}\Lambda_{00}+F_{11}^m\Lambda_{20}-F_{33}^m\Lambda_{00} \quad (63)$$

$$K_3^H = -\frac{(A_{31}^m)^2}{A_{11}}\Lambda_{00} + X_{11}^m\Lambda_{20} - X_{33}^m\Lambda_{00} \quad (64)$$

$$M = -I_0\Lambda_{00} + (ea)^2 I_0\Lambda_{20} + I_2\Lambda_{20} - (ea)^2 I_2\Lambda_{40} \quad (65)$$

where

$$\begin{aligned}
\Lambda_{00} &= \int_0^L X_m X_m dx, \quad \Lambda_{20} = \int_0^L X_m'' X_m dx \\
\Lambda_{40} &= \int_0^L X_m'''' X_m dx, \quad \Lambda_{11} = \int_0^L X_m' X_m' dx \\
\tilde{\Lambda}_{00} &= \int_0^L (X_m)^4 dx, \quad \Xi_{11} = \int_0^L R_m' X_m' dx \\
\Gamma_{20} &= \int_0^L R_m'' R_m dx, \quad \Gamma_{40} = \int_0^L R_m'''' R_m dx
\end{aligned} \quad (66)$$

By using last two relations in Eq. (52), components Φ_m and Υ_m can be calculated as

$$\begin{aligned}
&\Phi_m = Z_1 W_m + Z_2 W_m^2, \quad \Upsilon_m = Z_3 W_m + Z_4 W_m^2 \\
&Z_1 = -\frac{(K_2^H K_3^S - K_3^H K_2^S)}{K_3^E K_2^H - K_2^E K_3^H}, \quad Z_2 = -\frac{(G_3 K_2^H - G_2 K_3^H)}{K_3^E K_2^H - K_2^E K_3^H} \\
&Z_3 = -\frac{(K_3^E K_2^S - K_2^E K_3^S)}{K_3^E K_2^H - K_2^E K_3^H}, \quad Z_4 = -\frac{+(G_2 K_3^E - G_3 K_2^E)}{K_3^E K_2^H - K_2^E K_3^H}
\end{aligned} \quad (67)$$

Placing gained relations of Eq. (67) in 1st equation of Eq. (52) leads to

$$\begin{aligned}
&\frac{K^*}{M}W + \frac{G_1}{M}W^3 + \frac{Z^*}{M}W^2 + \ddot{W} \\
&= \frac{F_{elliptic}}{M} cn(\psi t, k_f^2)
\end{aligned} \quad (68)$$

where

$$\begin{aligned}
K^* &= K_1^S + K_1^E Z_1 + K_1^H Z_3 \\
Z^* &= K_1^E Z_2 + K_1^H Z_4
\end{aligned} \quad (69)$$

For solving the non-linear governing equation, the maximum deflection (W) can be approximated via Jacobi elliptic function (cn) as (Liu *et al*. 2001).

$$W = \widetilde{W} cn(\psi t, k^2) \quad (70)$$

Here, k^2 denotes the modulus of the elliptic function; $\widetilde{W}$ denotes vibrational amplitude. The Jacobi elliptic function (cn) can be written in series of trigonometric form as a function of complete elliptic integral of the first kind K(k) as

$$cn(\omega t, k^2) = \frac{2\pi}{kK}\sum_{r=0}^{\infty}\frac{q^{r+\frac{1}{2}}}{1+q^{2r+1}} cos\left((2r+1)\frac{\pi\psi t}{2K}\right) \quad (71)$$

Here, $q = exp(-\pi K'/K)$ and $K' = K(l)$ denotes the associated complete elliptic integral of the first kind and

$$K = \int_0^{\pi/2}\frac{d\theta}{\sqrt{1-k^2 sin^2\theta}} \quad (72)$$

Then, inserting Eq. (71) into Eq. (68) and with the use of series expansion for $cn|cn| \approx a_0 cn + a_1 cn^3$ one can obtain that

$$\begin{aligned}
&\widetilde{W}^3 + \frac{C_2\frac{K^*}{M} - (1-2k_f^2)C_2\psi^2 - 2k_f^2\psi^2 C_4}{C_4\frac{G_1}{M}}\widetilde{W} \\
&-\frac{FC_2}{G_1 C_4} = 0
\end{aligned} \quad (73)$$

$$k^2 = \frac{\frac{K^*}{M}|\bar{W}|a_1 + \frac{G_1}{M}\bar{W}^2}{2\left(\frac{K^*}{M} + \frac{Z^*}{M}|\bar{W}|(a_0+a_1) + \frac{G_1}{M}\bar{W}^2\right)} \quad (74)$$

where

$$C_2 = \int_0^{4K(k)} cn^2\, d\psi \quad (75)$$

$$\begin{aligned}
C_{2r+2} &= \int_0^{4K(k)} cn^{2r+2}\, d\psi \\
&= \frac{2r(2k^2-1)C_{2r} + (2r-1)(1-k^2)C_{2r-2}}{(2r+1)k^2}, \\
r &= 1,2,3,..
\end{aligned} \quad (76)$$

Also, dimensionless quantities are selected as

$$\begin{aligned}
&K_L = k_L\frac{L^4}{D_{11}}, \quad K_p = k_p\frac{L^2}{D_{11}}, \quad K_{NL} = k_{NL}\frac{L^4}{A_{11}} \\
&\tilde{\omega} = \psi L^2\sqrt{\frac{\rho A}{\tilde{c}_{11} I}}, \quad \mu = \frac{ea}{L}
\end{aligned} \quad (77)$$

5. Obtained results and discussion

Throughout the present section, several graphical examples have been presented and also obtained results have been discussed to survey the correctness of the presented theory in evaluating the free vibrational properties of multi-phase MEE nano-size beams. Obtained results have been provided from the geometrically perfect assumption for the nanobeam. The magnitude of length for nano-scale beam has been chosen to be L = 10 nm. For corroborating the reliability of the presented approach, the obtained findings have been compared with the work of Li *et al.* (2018) for the non-linear vibration frequencies of imperfect nanobeam based on a variety of maximum vibration amplitude ($\widetilde{W}$) presented in Table 2. One can observe that the results are in accordance with those provided by Li *et al.* (2018) which demonstrate the efficient of the present model. A comparison between approximate and exact solutions for non-linear vibration frequency at

Table 2 Validation of nonlinear vibration frequency for nanobeams

$\widetilde{W}$ = 0.2	Li *et al.* (2018)	9.9065
	Present	9.9065
$\widetilde{W}$ = 0.4	Li *et al.* (2018)	10.0166
	Present	10.0166

Table 3 Comparison between approximate and exact solutions for non-linear vibration frequency at different values of normalized amplitude (L/h = 20)

	$\frac{\widetilde{W}}{h}=0.5$	$\frac{\widetilde{W}}{h}=0.6$	$\frac{\widetilde{W}}{h}=0.7$	$\frac{\widetilde{W}}{h}=0.8$	$\frac{\widetilde{W}}{h}=0.9$
Approximate solution	26.2198	27.2925	28.6134	29.8191	31.2421
Exact solution	26.1998	27.2571	28.4420	29.7388	31.1334

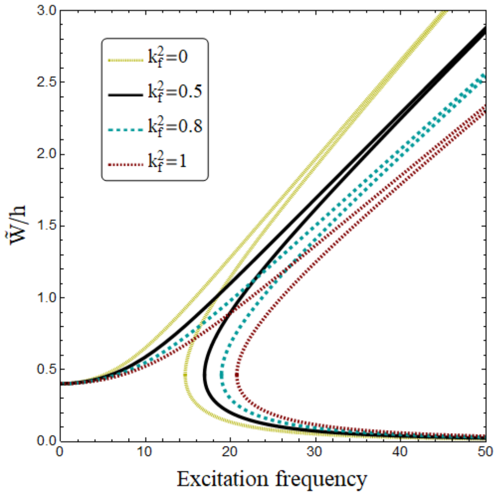

Fig. 2 Effect of the modulus of the Jacobi elliptic function on vibration frequency curves of the nanobeam (L/h = 20, V_f = 20%, $\tilde{F}$ = 0.01, V_E = 0, Ω = 0)

different values of normalized amplitude has been presented in Table 3. In this table the dimensionless nonlocal parameter is set to μ = 0.2. As can be seen, approximate solution gives larger frequencies than exact solution due to ignoring higher harmonics. In the following, exact solution will be used for presenting obtained results.

In Fig. 2, the effect of the modulus of elliptic function (k_f^2) on frequency-amplitude curves of a MEE nanobeam is presented assuming that the force magnitude is $\tilde{F}$ = 0.01 and nonlocal factors is set to μ = 0.2. It is well known that the nonlinear vibrational frequencies of a beam are independent of the normalized amplitude of their corresponding mode shapes in the cases of linear vibration behavior, while they are dependent upon the normalized amplitude of their corresponding mode shapes in the cases of geometrical nonlinear behavior, which often occurs when the vibrational amplitude of the mode shape approaches the total thickness of the beam. However, the frequency-amplitude curve has a jump when the excitation frequencies reaches the natural frequency. It is shown that natural frequency and magnitude of beam deflection are dependent on the modulus of elliptic force function. It is clear that the higher the modulus k_f, the lower the amplitude for certain frequencies. Moreover, the jump is shifted to higher frequencies for the higher values of the modulus. It must be stated that when k_f = 0, the elliptic force reduces to a simple trigonometric force with single excitation.

Showed in Fig. 3 is the efficacy of exerted load magnitude on deflection-frequency curve of multi-phase MEE nano-scale beams under an excitation of elliptic type with k_f^2 = 0.5. Based on this figure, one may understand that the shift frequencies are un-varied by the increasing in force magnitude. It can be explained that the frequency is only dependent on effective linear stiffness and mass density of the nano-scale beam. Therefore, the shift frequency is not influenced by exerted dynamic load. Yet, non-dimension deflection of the nano-scale beam goes larger via applying a greater load.

Fig. 4 indicates the efficacy of the small scales on the non-linear vibrational frequency of two-phase MEE nano-size beam versus normalized vibrational amplitudes ($\widetilde{W}/h$). It may be seen that as the dimensionless nonlocal parameter (μ) enhances, the normalized shift frequency declines. Afterwards, it may be deduced that the classical elastic (i.e., the local) theory, which does not incorporate the small size

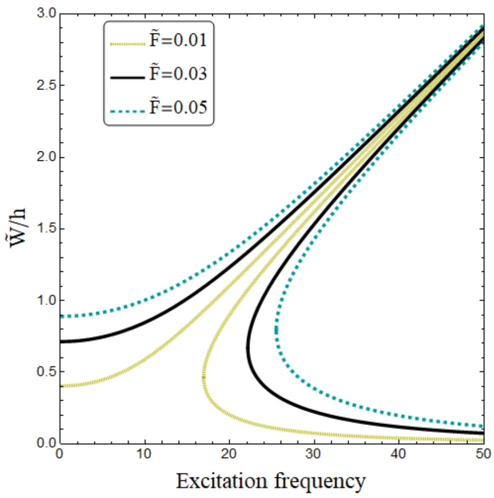

Fig. 3 Effect of force magnitude on vibration frequency curves of the nanobeam (L/h = 20, V_f = 20%, V_E = 0, Ω = 0, k^2_f = 0.5)

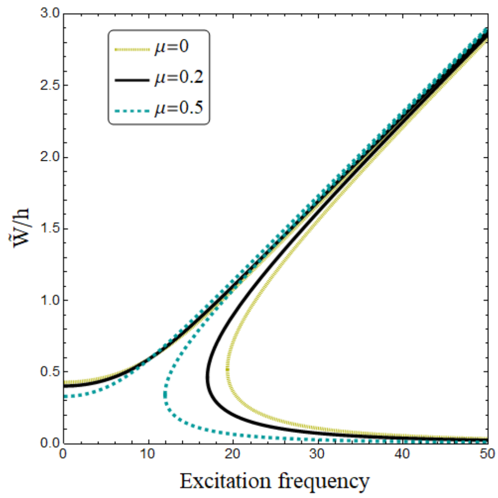

Fig. 4 Effect of dimensionless nonlocal factor on vibration frequency curves of the nanobeam (L/h = 20, V_f = 20%, V_E = 0, k^2_f = 0.5, Ω = 0)

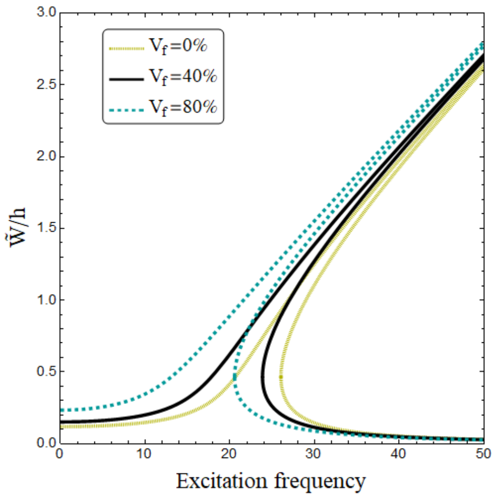

(a) $V_E = +0.01$ V

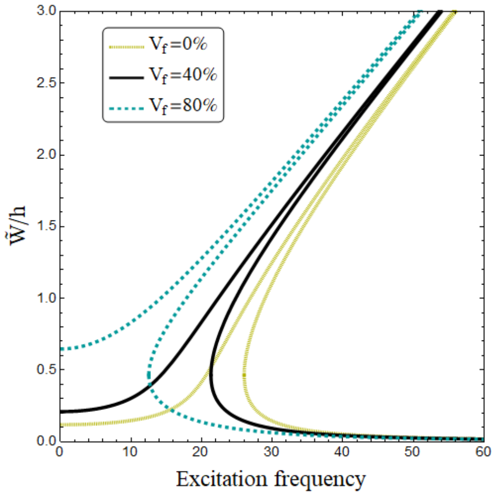

(b) $V_E = +0.01$ V

Fig. 5 Effect of piezoelectric percentage and electric voltage on vibration frequency curves of the nanobeam ($\mu = 0.2$, $\Omega = 0$, $k^2_f = 0.5$, $K_L = 100$, $K_P = 20$, $K_{NL} = 0$)

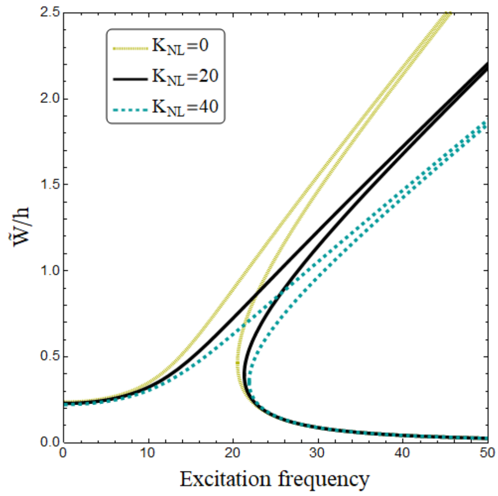

(a) $K_L = 100$, $K_P = 0$

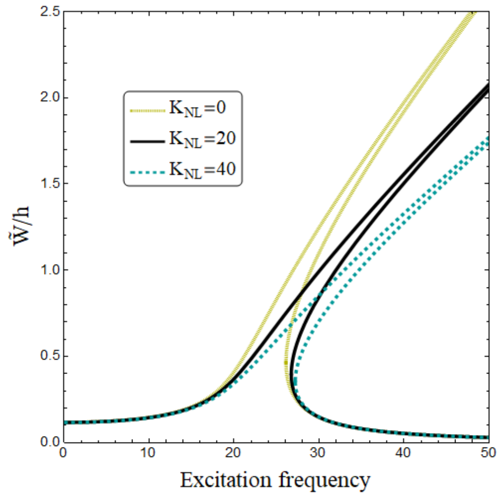

(b) $K_L = 100$, $K_P = 20$

Fig. 6 Effect of elastic foundation parameters on vibration frequency curves of the nanobeam ($V_f = 20\%$, $\mu = 0.2$, $k^2_f = 0.5$, $V_E = 0$, $\Omega = 0$)

impacts, will provide the higher approximations for the normalized vibrational frequency. However, the nonlocal continuum mechanics will give more precise and dependable results.

Combined influences of exerted electrical voltage and piezoelectric volume on forced vibrational curves of the nanobeam is shown in Fig. 5 considering $\tilde{F} = 0.01$. The volume of piezoelectric ingredient has been selected to be V_f = 0%, 40% and 80%. From the figure, it may be understood that enhancing the volume of piezoelectric ingredient yields lower shift frequencies. This is associated with the decrement in the elastic stiffness of nano-scale beams by increasing in piezoelectric portion. Afterwards, the elastic modulus of composites decreases by increasing in piezoelectric ingredient as presented in Table 1. Also, as the magnitude of electric voltage is lower, the curves are closer to each other. Accordingly, a MEE nano-scale beam with higher percentages of piezoelectric ingredient is more susceptible to the induced electrical fields.

Non-dimension deflection of MEE nano-scale beam against non-dimension excitation frequency has been displayed in Fig. 6 based on diverse substrate coefficients (K_L, K_P, K_{NL}). The amplitude of exerted force is chosen as $\tilde{F} = 0.01$ and the piezoelectric ingredient volume is chosen as V_f = 20%. One may observe that growth of linear (K_L) and shear (K_P) substrate coefficients makes the MEE nano-size beam more rigid leading to greater natural frequencies. As regards, nonlinear substrate coefficient has no influence on the measure of natural frequencies. However, enlarging the values of K_{NL} yields more tendency of frequency-deflection curves to the right. This means that the hardening influences of geometrical nonlinearity become more announced with increase of K_{NL}.

Changes of non-linear vibration frequency versus normalized amplitude in various electric voltage (V_E) and magnetic field intensity (Ω) are respectively presented in Figs. 7 and 8. One can observe that the non-linear shift frequency reduces via changing of applied field from negative to positive voltages. As seen, if magnetic field intensity is increased from negative to positive, non-linear

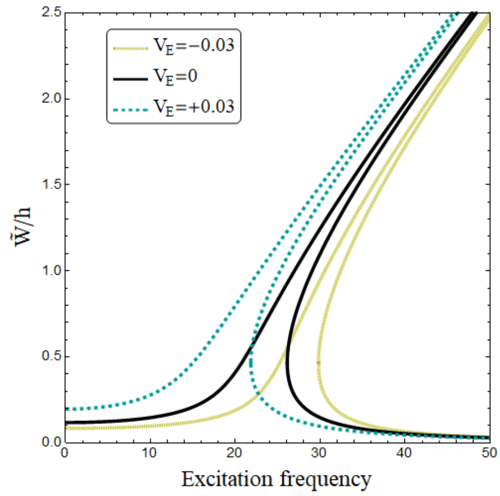

Fig. 7 Effect of applied voltage on vibration frequency curves of the nanobeam (V_f = 20%, μ = 0.2, K_L = 100, K_P = 20, Ω = 0)

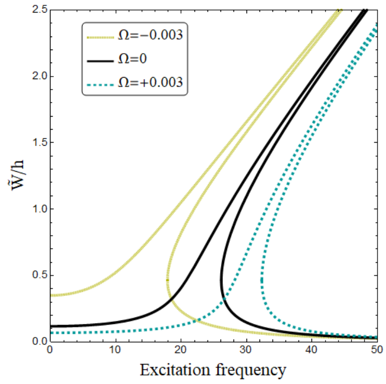

Fig. 8 Effect of magnetic field intensity on vibration frequency curves of the nanobeam (V_f = 20%, μ = 0.2, V_E = 0, K_L = 100, K_P = 20, K_{NL} = 0)

vibration frequency is increased. The reason of this behavior is that MEE material has the ability to absorb magnetism and keep it and by rising magnetic field intensity, this ability shows own more. Such materials are capable to convert force of magnetic potential to mechanical force. Thus, via the growth of field intensity, non-linear vibration frequency enlarges because magnetic field creates tensile forces in nanobeam.

6. Conclusions

The presented research examined nonlocal non-linear forced vibration frequency of two-phase MEE nanobeams under elliptic-type excitation by presenting an exact solution using Jacobi elliptic functions. The nanobeam was assumed to be rested on elastic foundation with three parameters including linear, shear and nonlinear. It was seen that as the dimensionless nonlocal parameter increases, the normalized shift frequency decreases. Thus, it can be deduced that the classical elastic (i.e., the local) model, which does not consider the small-scale impacts, will give higher approximations for the non-dimension vibrational frequency. However, impact of non-linear foundation parameter on vibration frequency curves has an increasing trend with increasing in vibration amplitude. Also, magnetic field effect on vibration characteristics of MEE nanobeams relies on the value of piezoelectric volume. But, the rate of frequency increment versus magnetic field intensity becomes lower by increase of piezoelectric volume. It was found that the higher the modulus k_f, the lower the amplitude for certain frequencies. Moreover, the jump is shifted to higher frequencies for the higher values of the modulus.

Acknowledgments

The first and second authors would like to thank FPQ (Fidar project Qaem) for providing the fruitful and useful help.

References

Abualnour, M., Chikh, A., Hebali, H., Kaci, A., Tounsi, A., Bousahla, A.A. and Tounsi, A. (2019), “Thermomechanical analysis of antisymmetric laminated reinforced composite plates using a new four variable trigonometric refined plate theory”, *Comput. Concrete*, *Int. J.*, **24**(6), 489-498. https://doi.org/10.12989/cac.2019.24.6.489

Addou, F.Y., Meradjah, M., Bousahla, A.A., Benachour, A., Bourada, F., Tounsi, A. and Mahmoud, S.R. (2019), “Influences of porosity on dynamic response of FG plates resting on Winkler/Pasternak/Kerr foundation using quasi 3D HSDT”, *Comput. Concrete*, *Int. J.*, **24**(4), 347-367. https://doi.org/10.12989/cac.2019.24.4.347

Ahmed, R.A., Fenjan, R.M. and Faleh, N.M. (2019), “Analyzing post-buckling behavior of continuously graded FG nanobeams with geometrical imperfections”, *Geomech. Eng.*, *Int. J.*, **17**(2), 175-180. https://doi.org/10.12989/gae.2019.17.2.175

Akbaş, S.D. (2016), “Forced vibration analysis of viscoelastic nanobeams embedded in an elastic medium”, *Smart Struct. Syst.*, *Int. J.*, **18**(6), 1125-1143. https://doi.org/10.12989/sss.2016.18.6.1125

Alasadi, A.A., Ahmed, R.A. and Faleh, N.M. (2019), “Analyzing nonlinear vibrations of metal foam nanobeams with symmetric and non-symmetric porosities”, *Adv. Aircr. Spacecr. Sci.*, *Int. J.*, **6**(4), 273-282. https://doi.org/10.12989/aas.2019.6.4.273

Alimirzaei, S., Mohammadimehr, M. and Tounsi, A. (2019), “Nonlinear analysis of viscoelastic micro-composite beam with geometrical imperfection using FEM: MSGT electro-magneto-elastic bending, buckling and vibration solutions”, *Struct. Eng. Mech.*, *Int. J.*, **71**(5), 485-502. https://doi.org/10.12989/sem.2019.71.5.485

Al-Maliki, A.F., Faleh, N.M. and Alasadi, A.A. (2019), “Finite element formulation and vibration of nonlocal refined metal foam beams with symmetric and non-symmetric porosities”, *Struct. Monit. Maint.*, *Int. J.*, **6**(2), 147-159. https:// doi.org/10.12989/smm.2019.6.2.147

Annigeri, A.R., Ganesan, N. and Swarnamani, S. (2007), “Free vibration behaviour of multiphase and layered magneto-electro-elastic beam”, *J. Sound Vib.*, **299**(1-2), 44-63. https://doi.org/10.1016/j.jsv.2006.06.044

Aydogdu, M., Arda, M. and Filiz, S. (2018), “Vibration of axially functionally graded nano rods and beams with a variable nonlocal parameter”, *Adv. Nano Res.*, *Int. J.*, **6**(3), 257-278. https://doi.org/10.12989/anr.2018.6.3.257

Azimi, M., Mirjavadi, S.S., Shafiei, N. and Hamouda, A.M.S. (2017), "Thermo-mechanical vibration of rotating axially functionally graded nonlocal Timoshenko beam", *Appl. Phys. A*, **123**(1), 104. https://doi.org/10.1007/s00339-016-0712-5

Azimi, M., Mirjavadi, S.S., Shafiei, N., Hamouda, A.M.S. and Davari, E. (2018), "Vibration of rotating functionally graded Timoshenko nano-beams with nonlinear thermal distribution", *Mech. Adv. Mater. Struct.*, **25**(6), 467-480. https://doi.org/10.1080/15376494.2017.1285455

Balubaid, M., Tounsi, A., Dakhel, B. and Mahmoud, S.R. (2019), "Free vibration investigation of FG nanoscale plate using nonlocal two variables integral refined plate theory", *Comput. Concrete*, *Int. J.*, **24**(6), 579-586. https://doi.org/10.12989/cac.2019.24.6.579

Barati, M.R. (2017), "Coupled effects of electrical polarization-strain gradient on vibration behavior of double-layered flexoelectric nanoplates", *Smart Struct. Syst.*, *Int. J.*, **20**(5), 573-581. https://doi.org/10.12989/sss.2017.20.5.573

Batou, B., Nebab, M., Bennai, R., Atmane, H.A., Tounsi, A. and Bouremana, M. (2019). "Wave dispersion properties in imperfect sigmoid plates using various HSDTs", *Steel Compos. Struct.*, *Int. J.*, **3**(5), 699-716. https://doi.org/10.12989/scs.2019.33.5.699

Bedia, A., Houari, M.S.A., Bessaim, A., Bousahla, A.A., Tounsi, A., Saeed, T. and Alhodaly, M.S. (2019), "A new hyperbolic two-unknown beam model for bending and buckling analysis of a nonlocal strain gradient nanobeams", *J. Nano Res.*, **57**, 175-191. https://doi.org/10.4028/www.scientific.net/JNanoR.57.175

Belbachir, N., Draich, K., Bousahla, A.A., Bourada, M., Tounsi, A. and Mohammadimehr, M. (2019), "Bending analysis of anti-symmetric cross-ply laminated plates under nonlinear thermal and mechanical loadings", *Steel Compos. Struct.*, *Int. J.*, **33**(1), 81-92. https://doi.org/10.12989/scs.2019.33.1.081

Benmansour, D.L., Kaci, A., Bousahla, A.A., Heireche, H., Tounsi, A., Alwabli, A.S. and Mahmoud, S.R. (2019), "The nano scale bending and dynamic properties of isolated protein microtubules based on modified strain gradient theory", *Adv. Nano Res.*, *Int. J.*, **7**(6), 443-457. https://doi.org/10.12989/anr.2019.7.6.443

Berghouti, H., Bedia, A.E.A., Benkhedda, A. and Tounsi, A. (2019). "Vibration analysis of nonlocal porous nanobeams made of functionally graded material", *Adv. Nano Res.*, *Int. J.*, **7**(5), 351-364. https://doi.org/10.12989/anr.2019.7.5.351

Besseghier, A., Heireche, H., Bousahla, A.A., Tounsi, A. and Benzair, A. (2015), "Nonlinear vibration properties of a zigzag single-walled carbon nanotube embedded in a polymer matrix", *Adv. Nano Res.*, *Int. J.*, **3**(1), 29-37. https://doi.org/10.12989/anr.2015.3.1.029

Boukhlif, Z., Bouremana, M., Bourada, F., Bousahla, A.A., Bourada, M., Tounsi, A. and Al-Osta, M.A. (2019), "A simple quasi-3D HSDT for the dynamics analysis of FG thick plate on elastic foundation", *Steel Compos. Struct.*, *Int. J.*, **31**(5), 503-516. https://doi.org/10.12989/scs.2019.31.5.503

Boulefrakh, L., Hebali, H., Chikh, A., Bousahla, A.A., Tounsi, A. and Mahmoud, S.R. (2019), "The effect of parameters of visco-Pasternak foundation on the bending and vibration properties of a thick FG plate", *Geomech. Eng.*, *Int. J.*, **18**(2), 161-178. https://doi.org/10.12989/gae.2019.18.2.161

Bounouara, F., Benrahou, K.H., Belkorissat, I. and Tounsi, A. (2016), "A nonlocal zeroth-order shear deformation theory for free vibration of functionally graded nanoscale plates resting on elastic foundation", *Steel Compos. Struct.*, *Int. J.*, **20**(2), 227-249. https://doi.org/10.12989/scs.2016.20.2.227

Bourada, F., Bousahla, A.A., Bourada, M., Azzaz, A., Zinata, A. and Tounsi, A. (2019), "Dynamic investigation of porous functionally graded beam using a sinusoidal shear deformation theory", *Wind Struct.*, *Int. J.*, **28**(1), 19-30. https://doi.org/10.12989/was.2019.28.1.019

Boutaleb, S., Benrahou, K.H., Bakora, A., Algarni, A., Bousahla, A.A., Tounsi, A., Tounsi, A. and Mahmoud, S.R. (2019), "Dynamic Analysis of nanosize FG rectangular plates based on simple nonlocal quasi 3D HSDT", *Adv. Nano Res.*, *Int. J.*, **7**(3), 189-206. https://doi.org/10.12989/anr.2019.7.3.191

Chaabane, L.A., Bourada, F., Sekkal, M., Zerouati, S., Zaoui, F. Z., Tounsi, A., Derras, A., Bousahla, A.A. and Tounsi, A. (2019), "Analytical study of bending and free vibration responses of functionally graded beams resting on elastic foundation", *Struct. Eng. Mech.*, *Int. J.*, **71**(2), 185-196. https://doi.org/10.12989/sem.2019.71.2.185

Chaudhary, S., Sahu, S.A. and Singhal, A. (2017), "Analytic model for Rayleigh wave propagation in piezoelectric layer overlaid orthotropic substratum", *Acta Mechanica*, **228**(2), 495-529. https://doi.org/10.1007/s00707-016-1708-0

Dehghan, M. and Ebrahimi, F. (2018), "On wave dispersion characteristics of magneto-electro-elastic nanotubes considering the shell model based on the nonlocal strain gradient elasticity theory. *Eur. Phys. J. Plus*, **133**(11), 466. https://doi.org/10.1140/epjp/i2018-12304-7

Draiche, K., Bousahla, A.A., Tounsi, A., Alwabli, A.S., Tounsi, A. and Mahmoud, S.R. (2019), "Static analysis of laminated reinforced composite plates using a simple first-order shear deformation theory", *Comput. Concrete*, *Int. J.*, **24**(4), 369-378. https://doi.org/10.12989/cac.2019.24.4.369

Draoui, A., Zidour, M., Tounsi, A. and Adim, B. (2019), "Static and dynamic behavior of nanotubes-reinforced sandwich plates using (FSDT)", *J. Nano Res.*, **57**, 117-135. https://doi.org/10.4028/www.scientific.net/JNanoR.57.117

Ebrahimi, F. and Barati, M.R. (2016), "A nonlocal higher-order refined magneto-electro-viscoelastic beam model for dynamic analysis of smart nanostructures", *Int. J. Eng. Sci.*, **107**, 183-196. https://doi.org/10.1016/j.ijengsci.2016.08.001

Eltaher, M.A., Emam, S.A. and Mahmoud, F.F. (2012), "Free vibration analysis of functionally graded size-dependent nanobeams", *Appl. Math. Comput.*, **218**(14), 7406-7420. https://doi.org/10.1016/j.amc.2011.12.090

Eshraghi, I., Jalali, S.K. and Pugno, N.M. (2016), "Imperfection sensitivity of nonlinear vibration of curved single-walled carbon nanotubes based on nonlocal timoshenko beam theory", *Materials*, **9**(9), 786. https://doi.org/10.3390/ma9090786

Eringen, A.C. (1972), "Linear theory of nonlocal elasticity and dispersion of plane waves", *Int. J. Eng. Sci.*, **10**(5), 425-435. https://doi.org/10.1016/0020-7225(72)90050-X

Farajpour, A., Yazdi, M.H., Rastgoo, A., Loghmani, M. and Mohammadi, M. (2016), "Nonlocal nonlinear plate model for large amplitude vibration of magneto-electro-elastic nanoplates", *Compos. Struct.*, **140**, 323-336. https://doi.org/10.1016/j.compstruct.2015.12.039

Fenjan, R.M., Ahmed, R.A., Alasadi, A.A. and Faleh, N.M. (2019), "Nonlocal strain gradient thermal vibration analysis of double-coupled metal foam plate system with uniform and non-uniform porosities", *Coupl. Syst. Mech.*, *Int. J.*, **8**(3), 247-257. https://doi.org/10.12989/csm.2019.8.3.247

Guo, J., Chen, J. and Pan, E. (2016), "Static deformation of anisotropic layered magnetoelectroelastic plates based on modified couple-stress theory", *Compos. Part B Eng.*, **107**, 84-96. https://doi.org/10.1016/j.compositesb.2016.09.044

Hellal, H., Bourada, M., Hebali, H., Bourada, F., Tounsi, A., Bousahla, A.A. and Mahmoud, S.R. (2019), "Dynamic and stability analysis of functionally graded material sandwich plates in hygro-thermal environment using a simple higher shear deformation theory", *J. Sandw. Struct. Mater.* [In press] https://doi.org/10.1177/1099636219845841

Kaddari, M., Kaci, A., Bousahla, A.A., Tounsi, A., Bourada, F., Tounsi, A., Bedia, E.A.A. and Al-Osta, M.A. (2020), "A study on the structural behaviour of functionally graded porous plates on elastic foundation using a new quasi-3D model: bending and free vibration analysis", *Comput. Concrete*, *Int. J.*, **25**(1), 37-57. https://doi.org/10.12989/cac.2020.25.1.037

Ke, L.L., Wang, Y.S., Yang, J. and Kitipornchai, S. (2014), "The size-dependent vibration of embedded magneto-electro-elastic cylindrical nanoshells", *Smart Mater. Struct.*, **23**(12), 125036. https://doi.org/10.1088/0964-1726/23/12/125036

Kumaravel, A., Ganesan, N. and Sethuraman, R. (2007), "Buckling and vibration analysis of layered and multiphase magneto-electro-elastic beam under thermal environment", *Multidiscip. Model. Mater. Struct.*, **3**(4), 461-476. https://doi.org/10.1163/157361107782106401

Li, Y. and Shi, Z. (2009), "Free vibration of a functionally graded piezoelectric beam via state-space based differential quadrature", *Compos. Struct.*, **87**(3), 257-264. https://doi.org/10.1016/j.compstruct.2008.01.012

Li, L., Tang, H. and Hu, Y. (2018), "Size-dependent nonlinear vibration of beam-type porous materials with an initial geometrical curvature", *Compos. Struct.*, **184**, 1177-1188. https://doi.org/10.1016/j.compstruct.2017.10.052

Liu, S., Fu, Z., Liu, S. and Zhao, Q. (2001), "Jacobi elliptic function expansion method and periodic wave solutions of nonlinear wave equations", *Phys. Lett. A*, **289**(1-2), 69-74. https://doi.org/10.1016/S0375-9601(01)00580-1

Liu, H., Liu, H. and Yang, J. (2018), "Vibration of FG magneto-electro-viscoelastic porous nanobeams on visco-Pasternak foundation", *Compos. Part B Eng.*, **155**, 244-256. https://doi.org/10.1016/j.compositesb.2018.08.042

Mahesh, V. and Kattimani, S. (2019), "Finite element simulation of controlled frequency response of skew multiphase magneto-electro-elastic plates", *J. Intell. Mater. Syst. Struct.*, **30**(12), 1757-1771. https://doi.org/10.1177%2F1045389X19843674

Mahesh, V., Sagar, P.J. and Kattimani, S. (2018), "Influence of coupled fields on free vibration and static behavior of functionally graded magneto-electro-thermo-elastic plate", *J. Intell. Mater. Syst. Struct.*, **29**(7), 1430-1455. https://doi.org/10.1177%2F1045389X17740739

Mahesh, V., Kattimani, S., Harursampath, D. and Trung, N.T. (2019), "Coupled evaluation of the free vibration characteristics of magneto-electro-elastic skew plates in hygrothermal environment", *Smart Struct. Syst.*, *Int. J.*, **24**(2), 267-292. https://doi.org/10.12989/sss.2019.24.2.267

Mahmoudi, A., Benyoucef, S., Tounsi, A., Benachour, A., Bedia, A.E.A. and Mahmoud, S.R. (2019), "A refined quasi-3D shear deformation theory for thermo-mechanical behavior of functionally graded sandwich plates on elastic foundations", *J. Sandw. Struct. Mater.*, **21**(6), 1906-1926. https://doi.org/10.1177%2F1099636217727577

Mirjavadi, S.S., Rabby, S., Shafiei, N., Afshari, B.M. and Kazemi, M. (2017), "On size-dependent free vibration and thermal buckling of axially functionally graded nanobeams in thermal environment", *Appl. Phys. A*, **123**(5), 315. https://doi.org/10.1007/s00339-017-0918-1

Mirjavadi, S.S., Afshari, B.M., Barati, M.R. and Hamouda, A.M. S. (2018a), "Strain gradient based dynamic response analysis of heterogeneous cylindrical microshells with porosities under a moving load", *Mater. Res. Express*, **6**(3), 035029. https://doi.org/10.1088/2053-1591/aaf5a2

Mirjavadi, S.S., Afshari, B.M., Khezel, M., Shafiei, N., Rabby, S. and Kordnejad, M. (2018b), "Nonlinear vibration and buckling of functionally graded porous nanoscaled beams", *J. Brazil. Soc. Mech. Sci. Eng.*, **40**(7), 352. https://doi.org/10.1007/s40430-018-1272-8

Mirjavadi, S.S., Forsat, M., Hamouda, A.M.S. and Barati, M.R. (2019a), "Dynamic response of functionally graded graphene nanoplatelet reinforced shells with porosity distributions under transverse dynamic loads", *Mater. Res. Express*, **6**(7), 075045. https://doi.org/10.1088/2053-1591/ab1552

Mirjavadi, S.S., Afshari, B.M., Barati, M.R. and Hamouda, A.M.S. (2019b), "Transient response of porous FG nanoplates subjected to various pulse loads based on nonlocal stress-strain gradient theory", *Eur. J. Mech. A Solids*, **74**, 210-220. https://doi.org/10.1016/j.euromechsol.2018.11.004

Mirjavadi, S.S., Afshari, B.M., Barati, M.R. and Hamouda, A.M.S. (2019c), "Nonlinear free and forced vibrations of graphene nanoplatelet reinforced microbeams with geometrical imperfection", *Microsyst. Technol.*, **25**, 3137-3150. https://doi.org/10.1007/s00542-018-4277-4

Mirjavadi, S.S., Forsat, M., Barati, M.R., Abdella, G.M., Hamouda, A.M.S., Afshari, B.M. and Rabby, S. (2019d), "Post-buckling analysis of piezo-magnetic nanobeams with geometrical imperfection and different piezoelectric contents", *Microsyst. Technol.*, **25**(9), 3477-3488. https://doi.org/10.1007/s00542-018-4241-3

Mohammadi, H., Mahzoon, M., Mohammadi, M. and Mohammadi, M. (2014), "Postbuckling instability of nonlinear nanobeam with geometric imperfection embedded in elastic foundation", *Nonlinear Dyn.*, **76**(4), 2005-2016. https://doi.org/10.1007/s11071-014-1264-x

Mohammadimehr, M. and Alimirzaei, S. (2016), "Nonlinear static and vibration analysis of Euler-Bernoulli composite beam model reinforced by FG-SWCNT with initial geometrical imperfection using FEM", *Struct. Eng. Mech.*, *Int. J.*, **59**(3), 431-454. http://dx.doi.org/10.12989/sem.2016.59.3.431

Mokhtar, Y., Heireche, H., Bousahla, A.A., Houari, M.S.A., Tounsi, A. and Mahmoud, S.R. (2018), "A novel shear deformation theory for buckling analysis of single layer graphene sheet based on nonlocal elasticity theory", *Smart Struct. Syst.*, *Int. J.*, **21**(4), 397-405. https://doi.org/10.12989/sss.2018.21.4.397

Mouffoki, A., Bedia, E.A., Houari, M.S.A., Tounsi, A. and Mahmoud, S.R. (2017), "Vibration analysis of nonlocal advanced nanobeams in hygro-thermal environment using a new two-unknown trigonometric shear deformation beam theory", *Smart Struct. Syst.*, *Int. J.*, **20**(3), 369-383. https://doi.org/10.12989/sss.2017.19.2.115

Mutasim, S., Al-Qaisia, A.A. and Shatarat, N.K. (2017), "Nonlinear vibrations of a SWCNT with geometrical imperfection using nonlocal elasticity theory", *Modern Appl. Sci.*, **11**(10), 91.

Nan, C.W. (1994), "Magnetoelectric effect in composites of piezoelectric and piezomagnetic phases", *Phys. Rev. B*, **50**(9), 6082. https://doi.org/10.1103/PhysRevB.50.6082

Pan, E. and Han, F. (2005), "Exact solution for functionally graded and layered magneto-electro-elastic plates", *Int. J. Eng. Sci.*, **43**(3-4), 321-339. https://doi.org/10.1016/j.ijengsci.2004.09.006

Sahla, M., Saidi, H., Draiche, K., Bousahla, A.A., Bourada, F. and Tounsi, A (2019), "Free vibration analysis of angle-ply laminated composite and softcore sandwich plates", *Steel Compos. Struct.*, *Int. J.*, **33**(5), 663-679. https://doi.org/10.12989/scs.2019.33.5.663

Semmah, A., Heireche, H., Bousahla, A.A. and Tounsi, A. (2019), "Thermal buckling analysis of SWBNNT on Winkler foundation by non local FSDT", *Adv. Nano Res.*, *Int. J.*, **7**(2), 89-98. https://doi.org/10.12989/anr.2019.7.2.089

She, G.L., Yuan, F.G., Ren, Y.R., Liu, H.B. and Xiao, W.S. (2018), "Nonlinear bending and vibration analysis of functionally graded porous tubes via a nonlocal strain gradient theory", *Compos. Struct.*, **203**, 614-623. https://doi.org/10.1016/j.compstruct.2018.07.063

Thai, H.T. and Vo, T.P. (2012), "A nonlocal sinusoidal shear deformation beam theory with application to bending, buckling, and vibration of nanobeams", *Int. J. Eng. Sci.*, **54**, 58-66. https://doi.org/10.1016/j.ijengsci.2012.01.009

Tlidji, Y., Zidour, M., Draiche, K., Safa, A., Bourada, M., Tounsi, A., Bousahla, A.A. and Mahmoud, S.R. (2019), “Vibration analysis of different material distributions of functionally graded microbeam”, *Struct*. *Eng*. *Mech*., *Int*. *J*., **69**(6), 637-649. https://doi.org/10.12989/sem.2019.69.6.637

Vinyas, M. (2020a), “Computational analysis of smart magneto-electro-elastic materials and structures: review and classification”, *Arch*. *Comput*. *Methods Eng*., 1-44. https://doi.org/10.1007/s11831-020-09406-4

Vinyas, M. (2020b), “On frequency response of porous functionally graded magneto-electro-elastic circular and annular plates with different electro-magnetic conditions using HSDT”, *Compos*. *Struct*., **240**, 112044. https://doi.org/10.1016/j.compstruct.2020.112044

Vinyas, M. (2020c), “Interphase effect on the controlled frequency response of three-phase smart magneto-electro-elastic plates embedded with active constrained layer damping: FE study”, *Mater*. *Res*. *Express*, **6**(12), 125707. https://doi.org/10.1088/2053-1591/ab6649

Vinyas, M. and Kattimani, S.C. (2017a), “A finite element based assessment of static behavior of multiphase magneto-electro-elastic beams under different thermal loading”, *Struct*. *Eng*. *Mech*., *Int*. *J*., **62**(5), 519-535. https://doi.org/10.12989/sem.2017.62.5.519

Vinyas, M. and Kattimani, S.C. (2017b), “Static analysis of stepped functionally graded magneto-electro-elastic plates in thermal environment: a finite element study”, *Compos*. *Struct*., **178**, 63-86. https://doi.org/10.1016/j.compstruct.2017.06.068

Vinyas, M. and Kattimani, S.C. (2017c), “Hygrothermal analysis of magneto-electro-elastic plate using 3D finite element analysis”, *Compos*. *Struct*., **180**, 617-637. https://doi.org/10.1016/j.compstruct.2017.08.015

Vinyas, M. and Kattimani, S.C. (2017d), “A 3D finite element static and free vibration analysis of magneto-electro-elastic beam”, *Coupl*. *Syst*. *Mech*., *Int*. *J*., **6**(4), 465-485. https://doi.org/10.12989/csm.2017.6.4.465

Vinyas, M. and Kattimani, S.C. (2018), “Investigation of the effect of $BaTiO_3/CoFe_2O_4$ particle arrangement on the static response of magneto-electro-thermo-elastic plates”, *Compos*. *Struct*., **185**, 51-64. https://doi.org/10.1016/j.compstruct.2017.10.073

Vinyas, M., Sandeep, A.S., Nguyen-Thoi, T., Ebrahimi, F. and Duc, D.N. (2019a), “A finite element–based assessment of free vibration behaviour of circular and annular magneto-electro-elastic plates using higher order shear deformation theory”, *J Intell*. *Mater*. *Syst*. *Struct*., **30**(16), 2478-2501. https://doi.org/10.1177%2F1045389X19862386

Vinyas, M., Nischith, G., Loja, M.A.R., Ebrahimi, F. and Duc, N.D. (2019b), “Numerical analysis of the vibration response of skew magneto-electro-elastic plates based on the higher-order shear deformation theory”, *Compos*. *Struct*., **214**, 132-142. https://doi.org/10.1016/j.compstruct.2019.02.010

Vinyas, M., Harursampath, D. and Thoi, T.N. (2020), “A higher order coupled frequency characteristics study of smart magneto-electro-elastic composite plates with cut-outs using finite element methods”, *Def*. *Technol*. [In press] https://doi.org/10.1016/j.dt.2020.02.009

Yazid, M., Heireche, H., Tounsi, A., Bousahla, A.A. and Houari, M.S.A. (2018), “A novel nonlocal refined plate theory for stability response of orthotropic single-layer graphene sheet resting on elastic medium”, *Smart Struct*. *Syst*., *Int*. *J*., **21**(1), 15-25. https://doi.org/10.12989/sss.2018.21.1.015

Zaoui, F.Z., Ouinas, D. and Tounsi, A. (2019), “New 2D and quasi-3D shear deformation theories for free vibration of functionally graded plates on elastic foundations”, *Compos*. *Part B*, **159**, 231-247. https://doi.org/10.1016/j.compositesb.2018.09.051

Zarga, D., Tounsi, A., Bousahla, A.A., Bourada, F. and Mahmoud, S.R. (2019), “Thermomechanical bending study for functionally graded sandwich plates using a simple quasi-3D shear deformation theory”, *Steel Compos*. *Struct*., *Int*. *J*., **32**(3), 389-410. https://doi.org/10.12989/scs.2019.32.3.389

Zemri, A., Houari, M.S.A., Bousahla, A.A. and Tounsi, A. (2015), “A mechanical response of functionally graded nanoscale beam: an assessment of a refined nonlocal shear deformation theory beam theory”, *Struct*. *Eng*. *Mech*., *Int*. *J*., **54**(4), 693-710. https://doi.org/10.12989/sem.2015.54.4.693

CC